



# Association of histamine with hypertension-induced cardiac remodeling and reduction of hypertrophy with the histamine-2-receptor antagonist famotidine compared with the beta-blocker metoprolol

Ajay Godwin Potnuri<sup>1</sup> · Lingesh Allakonda<sup>2</sup> · Arulvelan Appavoo<sup>3</sup> · Sherin Saheera<sup>1</sup> · Renuka R. Nair<sup>1</sup>

Received: 18 September 2017 / Revised: 5 February 2018 / Accepted: 20 March 2018 / Published online: 11 October 2018  
© The Japanese Society of Hypertension 2018

## Abstract

The association of histamine with adverse cardiac remodeling in chronic pressure overload has not received much attention. A pilot study in spontaneously hypertensive rats (SHRs) indicated a reduction of left ventricular hypertrophy (LVH) with a histamine-2-receptor (H2R) antagonist (famotidine). This finding prompted a detailed investigation of temporal variation in myocardial histamine and H2R expression and the cardiovascular response to H2R antagonism compared with that of the conventional beta-blocker metoprolol. Reduction of LVH is known to reduce the risk of adverse cardiovascular events. The myocardial histamine content and H2R expression increased with age in SHRs but not in normotensive Wistar rats. The cardiovascular response to famotidine (30 mg kg<sup>-1</sup>) was compared with that of metoprolol (50 mg kg<sup>-1</sup>) in 6-month-old male SHRs treated for 60 days. The decrease in diastolic blood pressure and improvement in cardiac function induced by famotidine and metoprolol were comparable. Both treatments caused the regression of LVH as assessed from the hypertrophy index, histomorphometry, B type natriuretic peptide (BNP), pro-collagen 1, and hydroxyproline levels. Calcineurin-A expression (marker of pathological remodeling) decreased, and Peroxiredoxin-3 expression (mitochondrial antioxidant) increased in response to the treatments. The myocardial histamine levels decreased with the treatments. The age-dependent increase in myocardial histamine and H2R in the SHRs signifies their association with progressive cardiac remodeling. The regression of LVH and improvement in cardiac function by famotidine further demonstrates the role of histamine in cardiac remodeling. Hypertrophy of cultured cardiac cells upon exposure to histamine and the H2R agonist amthamine substantiates the role of histamine in cardiac remodeling. The cardiovascular response to famotidine is comparable to that of metoprolol, suggesting repurposing of H2R antagonists for the management of hypertensive heart disease.

**Keywords** Histamine · Histamine-2-receptor · H2R antagonist · Beta-blocker · Left ventricular hypertrophy

## Introduction

Left ventricular hypertrophy (LVH) is an adaptive outcome of uncontrolled hypertension. Nevertheless, LVH is an independent risk factor for cardiac failure [1] and sudden cardiac death [2]. Regression of LVH decreases the propensity for cardiac failure and adverse cardiovascular events [3], highlighting the need for identification of treatment strategies that mediate regression of hypertrophy together with a reduction of blood pressure. In cases of uncontrolled hypertension, activated sympathetic and renin-angiotensin-aldosterone systems are recognized as the major contributors to cardiac hypertrophy. Observations from a multi-ethnic study indicated that H2R blockers reduced the risk

---

✉ Renuka R. Nair  
renukanair52@gmail.com

<sup>1</sup> Division of Cellular and Molecular Cardiology, Sree Chitra Tirunal Institute for Medical Sciences and Technology, Thiruvananthapuram 695011, India

<sup>2</sup> Department of Pharmacology and Toxicology, National Institute of Pharmaceutical Education and Research, Hyderabad 500037 Telangana, India

<sup>3</sup> Department of Anesthesiology, Sree Chitra Tirunal Institute for Medical Sciences and Technology, Thiruvananthapuram 695011, India

for incidental heart failure, testifying to their importance in disease pathology [4]. Additionally, higher mast cell counts in the hearts of patients with cardiac hypertrophy [5], dilated cardiomyopathy and myocardial infarction [6] and increased circulating histamine levels in heart failure subjects substantiate the role of mast cells in cardiovascular pathophysiology [7]. Histamine-2-receptors (H2R), which are widely distributed in the myocardium, are known to mediate the cardiovascular effects of histamine [8]. In a rodent model, disruption of H2R inhibits the cardiac fibrosis and apoptosis precluding cardiac failure [9]. Under pathophysiological conditions, release of histamine by cardiac mast cells can activate H2R. However, the role of histamine in LVH and the use of H2R antagonists in regression of hypertrophy have not received much attention. In a genetic model of chronic pressure overload, we observed a decrease in the LV mass and wall thickness in response to H2R antagonism [10]. This preliminary observation prompted a detailed investigation of the temporal variation in myocardial histamine levels and H2R expression with the progression of hypertensive heart disease and the functional consequences of H2R antagonism. H2Rs share a unique structural homology with beta adrenoceptors [8]. Beta-blockers have cardio-protective effects and are widely used in the treatment of hypertension [11]. A comparison of H2R antagonism with that of the conventional  $\beta$ -blocker will help establish the effectiveness of the former in the management of hypertensive heart disease. Characterization of the cardiovascular consequence of H2R antagonism gains importance in view of the realization of the cardio-protective effects of this class of drug, because regression of hypertrophy can prevent progressive cardiac remodeling. Other than our own preliminary investigation, no reports have investigated the use of H2R antagonists for regression of hypertrophy. The above facts underscore the importance of a detailed inquiry into the structural, functional, and molecular changes in the heart consequent to treatment with H2R antagonists in comparison with a standard cardio-protective anti-hypertensive.

This study was designed with the objective of addressing the lacuna in the available information regarding the association of histamine and H2Rs with cardiac remodeling in hypertension and the role of H2R antagonism in the prevention of LVH. The spontaneously hypertensive rat (SHR) was selected as the experimental model, because it mimics the cardiovascular changes associated with chronic human hypertension [12]. To examine whether the histamine levels and H2R expression increased with progressive cardiac remodeling, age-associated changes in the myocardial histamine levels were examined in 1-month, 6-month, and 12-month-old SHRs. The functional consequence of treatment with a H2R blocker (famotidine) was studied in 6-month-old SHRs because they represent the stable and

adaptive phase of hypertrophy [13]. The cardiovascular response to H2R antagonism was compared with that of a conventionally used beta-blocker (metoprolol tartrate) based on assessment of structural, functional and molecular characteristics associated with maladaptive cardiac remodeling.

Identification of a positive cardiovascular response to H2R antagonism is expected to provide a complimentary approach for the management of hypertension and cardiac hypertrophy.

## Methods

### Animals and chemicals

All animal care and experimental procedures for this study were approved by the Institutional Animal Ethics Committee based on the Guidelines of the Committee for the Purpose of Control and Supervision of Experiments on Animals (CPCSEA). Male SHR and Wistar (WST) rats were used for the experiments. The animals were housed at 22 °C, maintained on a 12 h light-dark cycle, fed regular Rat Chow and had free access to drinking water. All chemicals used for the study were purchased from Sigma-Aldrich, India.

### Study design

Temporal variation in the myocardial histamine content and H2R expression was examined in 1-month, 6-month, and 12-month-old SHRs and WST rats. Six animals were studied per group. The ages correspond to the initial phase of hypertrophy, the stable phase of hypertrophy and the phase prior to failure [13]. To examine the cardiovascular response to the H2R antagonist famotidine, eighteen 6-month-old male SHRs were randomly assigned into three groups of six animals each. Famotidine was received as a gift from Intas Pharma Pvt. Ltd., India. Untreated SHRs served as a hypertensive control. One group received a daily oral dose of 30 mg kg<sup>-1</sup> day<sup>-1</sup> of famotidine for 60 days, and the positive control group was treated in parallel with a daily oral dose of 50 mg kg<sup>-1</sup> day<sup>-1</sup> of metoprolol tartrate, which is a known cardio-protective  $\beta$ -blocker. Metoprolol tartrate was purchased from Sigma-Aldrich (India). Six male WST rats served as the normo-tensive control. The metoprolol and famotidine doses were selected from previously published reports [14, 15, 16].

### Non-invasive blood pressure measurement and echocardiography

The blood pressure of the animals was recorded by warming them to 37 °C and placing the cuff at the base of the tail.

Three BP readings were recorded at 2-min intervals and averaged.

Transthoracic echocardiography was performed to evaluate the left ventricular function following a standard protocol [17, 18]. After anaesthetizing with ketamine [Ketalar-Parke Davis, India] ( $80 \text{ mg kg}^{-1}$ ) and xylazine [Brilliant Bio Pharmaceuticals, India] ( $20 \text{ mg kg}^{-1}$ ), the animals were placed in the left lateral decubitus position, and the echocardiographic measurements were performed using M mode, 2D, and Doppler imaging with the GE Vivid i with a 10-MHz linear transducer. Anesthetized animals were allowed to breathe spontaneously with oxygen supplementation through a nose cone. The ultrasound transducer probe was placed to obtain short-axis, long-axis, four-chamber, and apical cardiac views. The left ventricular end-diastolic diameter (LVEDD), left ventricular end-systolic diameter (LVESD), posterior wall thickness (PW) and septal wall thickness (IVS) during diastole were measured using M mode following the American Society of Echocardiography guidelines [19]. The LV mass (LVM), fractional shortening (FS), and relative wall thickness were calculated following standard protocols. The left ventricular end-systolic and end-diastolic areas were traced in a single-plane apical 4-chamber view, and the ejection fraction was calculated with the use of inbuilt software using the modified single-plane method (Simpson's rule). The mitral flow was recorded at the tip of the mitral valve from an apical view using Doppler imaging. Maximal velocities of the E and A waves were recorded, and the E/A ratio calculated. The isovolumic relaxation time (IVRT) was measured as the interval between the aortic closure click and the start of the mitral flow. The Tei index was calculated on the same apical view.

### Dissection of the heart and preparation of sera and tissue lysates

Blood was collected from the lateral tail vein, and sera were separated by centrifugation and stored at  $-80^\circ \text{C}$  prior to experimentation. The hearts were excised immediately and rinsed in ice-cold normal saline. Excess fluids were gently removed from the hearts using tissue paper, and then the hearts were weighed. The hearts were sampled for subsequent investigations. Mid-ventricular sections for histomorphometry were fixed in 10% neutral buffered formalin. Tissue samples for western blotting analysis were snap-frozen in liquid nitrogen and preserved at  $-80^\circ \text{C}$  prior to experimentation.

Tissue lysates were prepared by homogenization with radioimmunoprecipitation assay (RIPA) buffer (1:10 ratio). The homogenate was placed on ice for 30 min and centrifuged at  $5000\times g$  for 10 min at  $4^\circ \text{C}$ , and the supernatant was collected. The protein concentrations of the tissue lysates were estimated using the Bradford method.

### Myocardial histamine content

The myocardial histamine content was assessed as per the modified Shores method [20]. Briefly, the tissue lysates were extracted with n-butanol and alkalized with perchloric acid, followed by condensation with o-phthalaldehyde (OPT). Then, the fluorescence was measured in a spectrofluorometer (excitation 360 nm, emission 450 nm). The histamine levels were quantified and normalized to the protein concentration.

### Enzyme-linked immunosorbent assay

An enzyme-linked immunosorbent assay (ELISA) was performed to estimate the B type natriuretic peptide (BNP) and Pro-collagen I N-terminal peptide (PINP) levels in the sera and cardiac tissue lysates using commercially available kits.

### Myocardial hydroxyproline content

The myocardial hydroxyproline concentration was assessed according to the method of Reddy et al. with minor modifications [21]. A myocardial lysate from a pre-weighed tissue was hydrolyzed in HCl (6 M) for 4 h at  $110^\circ \text{C}$  and oxidized with chloramine T in acetate-citrate buffer (pH 6.0). Then, the mixture was incubated for 20 min at room temperature, and 20 volumes of Ehrlich's reagent was added. The samples were incubated at  $65^\circ \text{C}$  for 15 min, and the absorbance was measured spectrophotometrically at 550 nm. The results are expressed as  $\text{mg g}$  of wet tissue  $\text{weight}^{-1}$ .

### Expression of proteins associated with maladaptive cardiac remodeling

Myocardial protein expression was assessed by the western blotting. Total Akt (1:1000), phospho Akt at Ser 473 (1:1000), H2R (1:300), peroxiredoxin-3 (PRX3) (1:500), calcineurin-A (1:2000), and beta-actin (1:5000) were measured. The anti-H2R antibody was procured from Alomone Labs, Israel, and the remaining antibodies were procured from Abcam, India.

### Histomorphometry

Formalin-fixed mid-ventricular sections were dehydrated and embedded in paraffin. Tissue sections with a 5- $\mu\text{m}$  thicknesses was cut, deparaffinized, dehydrated, and stained with hematoxylin and eosin for general histomorphology or with picrosirius red for measurement of collagen deposition. The microscopic photographs were analyzed using the ImageJ software.

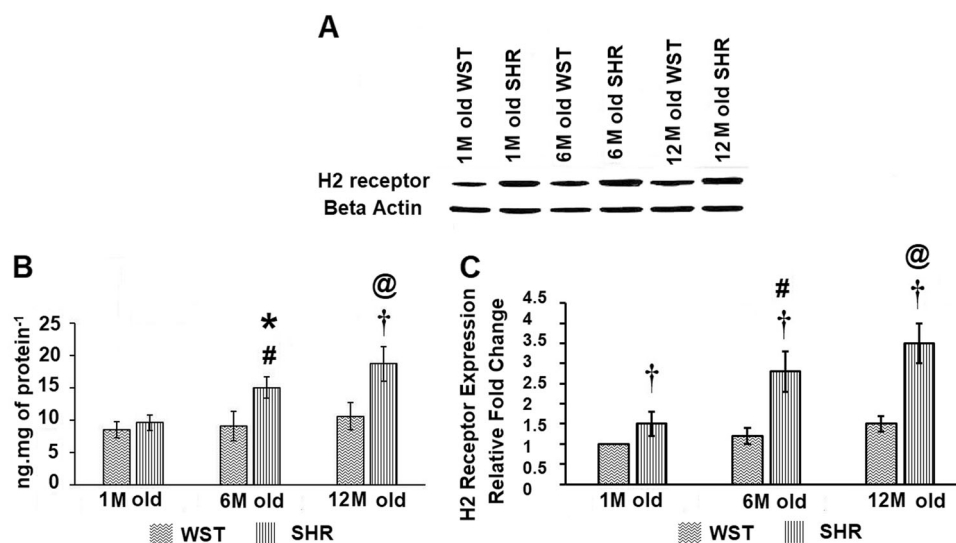


**Fig. 1** Temporal variation in the myocardial histamine content and H2R expression. **a** Representative photograph of an immunoblot showing H2R expression in SHRs and WST rats of different ages (1, 6, and 12 months) **b**. Graphical representation of temporal variation in the myocardial histamine content expressed as ng/mg protein **c**. Graphical representation of temporal variation in H2R expression as

arb.units. The data are presented as the mean  $\pm$  SD. 'M' denotes months. Variation was analyzed by one-way ANOVA followed by the Bonferroni post hoc test. \* $p < 0.05$  vs age-matched WST rats, † $p < 0.01$  vs age-matched WST rats, # $p < 0.01$  vs 1-month-old SHRs and @ $p < 0.001$  vs 1-month-old SHRs. ANOVA  $p < 0.01$  ( $n = 6$ /group)

### Delineation of the mechanism of action of histamine-mediated cardiomyocyte hypertrophy

Rat-derived H9c2 cardiocytes were procured from the National Center for Cell Science, Pune, India, and maintained in DMEM high-glucose medium supplemented with 10% fetal bovine serum. Cells were subjected to total serum deprivation for 24 h prior to experimentation and then exposed to either the H2R-specific agonist amthamine (5  $\mu$ M and 10  $\mu$ M) or histamine (10  $\mu$ M) for 48 h. To probe the rate of ERK phosphorylation, the cells were exposed for 12 h and collected after a thorough PBS washing step. Cellular proteins were isolated and used for the evaluation experiments. The protein content in the cell lysates was assessed with the Bradford method.

### Adenylate cyclase activity assay

Adenylate cyclase activity in the cell lysates was measured by quantifying the cyclic AMP concentrations [22]. Briefly, the total protein concentration of the cell lysates was adjusted to 2  $\mu$ g of protein  $\mu$ l<sup>-1</sup> in 10 mM Tris-HCl buffer (pH 7.4). ATP (final concentration 1 mM) was added to 250  $\mu$ l of the reaction mixture [100  $\mu$ l of cell lysate, 1 mM IBMX, 10 mM MgCl<sub>2</sub>, 0.4 mM EGTA, 10 mM creatine phosphate and 25 U of creatine kinase in 10 mM Tris-HCl (pH 7.4) preincubated at 30 °C for 15 min] and incubated for 10 min. The reaction was terminated by boiling for 5 min. The tubes were cooled and centrifuged at 12,000 $\times$ g for 5 min. The cAMP concentrations in the supernatants were measured using a

commercially available kit (Enzo Life Sciences, India) and expressed as nmoles of cAMP.mg protein<sup>-1</sup> min<sup>-1</sup>.

### Calcineurin activity assay

Calcineurin activity was assayed in the cell lysates using a commercially available kit based on the classic malachite green–inorganic phosphate assay (Enzo Life Sciences, India). The activity was calculated as nmol mg<sup>-1</sup> min<sup>-1</sup>.

### Statistical analysis

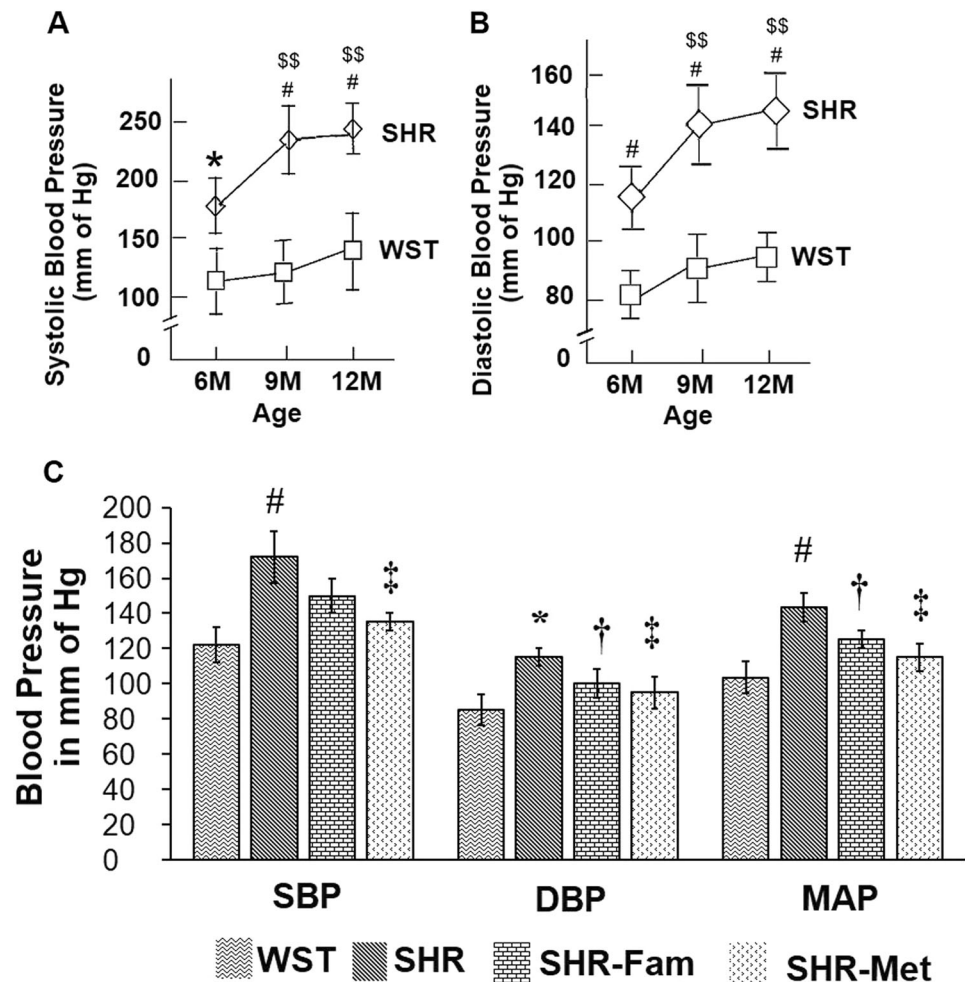
Values are expressed as the mean  $\pm$  SD. Variation between groups was determined using one-way analysis of variance (ANOVA) followed by comparisons between the treated and control groups using Bonferroni's post hoc test.  $P < 0.05$  was considered statistically significant.

## Results

### Temporal variation in the myocardial histamine content and H2R expression in SHRs

At 1 month of age, the myocardial histamine levels in the SHRs and WST rats were comparable (Fig. 1). An age-dependent increase in the myocardial histamine levels was observed in the SHRs; whereas, the histamine level remained unaltered in the WST rats. The levels in the 6-month-old animals were increased by 1.5-fold ( $p < 0.01$ )

**Fig. 2** Temporal variation in the blood pressure of SHRs and the response to treatment. **a** Temporal variation in systolic blood pressure of 6-, 9-, and 12-month-old SHRs compared with that of age- and sex-matched WST rats expressed as mmHg. **b** Temporal variation in diastolic blood pressure of 6-, 9-, and 12-month-old SHRs compared with that of age- and sex-matched WST rats expressed as mmHg. **c** Effect of famotidine on the systolic, diastolic, and mean blood pressures compared to the baseline blood pressure at initiation of treatment. The metoprolol-treated group served as a positive control. The data are presented as the mean  $\pm$  SD. 'M' denotes months. Variation was analyzed by one-way ANOVA followed by the Bonferroni post hoc test. \* $p < 0.05$  vs WST rats, # $p < 0.01$  vs WST rats, ‡ $p < 0.01$  vs SHRs, \$ $p < 0.01$  vs 6-month-old SHRs. ANOVA: Fig. 2a:  $p < 0.01$ , Fig. 2b:  $p < 0.01$  and Fig. 2c:  $p = 0.01$



and those in the 12-month-old animals were increased by twofold ( $p < 0.001$ ) compared to the levels in the 1-month-old animals. Compared to those of the age-matched Wistar rats, significantly higher myocardial histamine levels were observed in the SHRs at 6 and 12 months of age ( $p < 0.05$  and  $p < 0.001$ , respectively). Correspondingly, H2R expression as assessed by immunoblotting showed an age-dependent increase in the SHRs but remained unaltered in the WST rats. The expression levels were higher in the SHRs than those in the WST rats at all ages ( $p < 0.01$ ) (Fig. 1).

### Effect of famotidine and metoprolol on blood pressure and cardiac function

Blood pressure increased as a function of age in the SHRs and was significantly higher compared to that of the WST rats (SBP— $p < 0.01$ , DBP— $p < 0.01$ ) (Fig. 2a, b). Normalization of DBP was observed after famotidine and metoprolol treatment (Fig. 2c). A decrease in SBP was observed only with metoprolol ( $p < 0.01$  compared to the

untreated control). The decrease in DBP induced by metoprolol was relatively greater than that of famotidine. With a comparable heart rate (Table 1), the LV mass in the SHRs was higher than that in the WST rats ( $p < 0.01$ ) (Fig. 3b), which was normalized upon treatment with famotidine ( $p < 0.01$ ) and metoprolol ( $p < 0.01$ ). The LVDD in the SHRs was significantly lower than that in the WST rats ( $p < 0.05$ ) and improved with the treatments ( $p < 0.05$ ) (Table 1). The LVSD in the SHRs and WST rats was comparable and unaltered upon treatment (Table 1). The RWT in the SHRs was higher than that in the WST rats ( $p < 0.01$ ). The famotidine ( $p < 0.05$ ) and metoprolol ( $p < 0.05$ ) treatments reduced the RWT to the same extent (Table 1).

The LVESV in the SHRs was comparable to that of the WST rats and was unaffected by the treatments (Table 1). The LVEDV in the SHRs was lower than that of the WST rats ( $p < 0.01$ ) and improved significantly by the famotidine and metoprolol treatments ( $p < 0.01$ ) (Table 1). The ejection fraction (EF) in the SHRs was comparable to that of the WST rats and remained unaltered with the treatments (Fig. 3c). The FS in the SHRs was lower than that in the

**Table 1** Effect of famotidine treatment on cardiac function as evaluated by 2D-echocardiography

Variable	WST	SHR	SHR-Fam	SHR-Met	ANOVA <i>p</i> -value
Heart rate (beats/min)	345.8 ± 10.8	344.7 ± 14	350 ± 10	354 ± 7.3	0.4
LVDD (cm)	0.616 ± 0.03	0.545 ± 0.025*	0.591 ± 0.01 <sup>#</sup>	0.590 ± 0.021 <sup>#</sup>	0.01
LVSD (cm)	0.367 ± 0.02	0.283 ± 0.02*	0.285 ± 0.01	0.289 ± 0.009	0.001
FS (%)	40.5 ± 0.9	47.9 ± 3.3 <sup>‡</sup>	49.6 ± 3.6	49.4 ± 2.7	0.08
RWT	0.75 ± 0.002	0.84 ± 0.04 <sup>‡</sup>	0.77 ± 0.013*	0.76 ± 0.005*	0.001
LVEDV (ml)	0.81 ± 0.07	0.63 ± 0.025 <sup>‡</sup>	0.71 ± 0.017*	0.713 ± 0.02*	0.001
LVESV (ml)	0.040 ± 0.01	0.036 ± 0.01	0.0358 ± 0.009	0.0358 ± 0.006	0.808
E wave	63.8 ± 2.9	56.8 ± 3.2 <sup>‡</sup>	56.3 ± 1.7	56.3 ± 1.9	0.09
A wave	24.5 ± 2.2	33.7 ± 1.9 <sup>‡</sup>	28.8 ± 2.26*	28.9 ± 1.74*	0.001
IVRT	19.2 ± 1.829	22.7 ± 1 <sup>‡</sup>	19.9 ± 1.9*	18.7 ± 1*	0.001

The data are represented as mean ± SD. Variation between groups was analysed by one-way ANOVA followed by Bonferroni post hoc test

*A wave* peak trans mitral atrial filling velocity during late diastole, *E wave* peak early trans mitral filling velocity during early diastole, *FS* fractional shortening, *IVRT* iso volumetric relaxation time, *LVESV* left ventricular end-systolic volume, *LVEDV* left ventricular end-diastolic volume, *LVDD* left ventricular diameter during diastole, *LVSD* left ventricular diameter during systole

\**p* < 0.01 vs WST, <sup>#</sup>*p* < 0.01 vs SHR, and <sup>‡</sup>*p* < 0.05 vs WST

WST rats (*p* < 0.01) and remained unaffected by the treatments (Table 1).

Cardiac performance was evaluated by pulsed-wave Doppler assessment of mitral flow (Fig. 3a). A significant decrease in the E wave was observed in SHRs compared to that of the WST rats (*p* < 0.01), which was unaltered by the treatments. (Table 1). In the SHRs, the A wave was significantly increased compared to that of the WST rats (*p* < 0.01) and decreased significantly by the treatments (*p* < 0.01) (Table 1). The ratio between the E and A waves was significantly lower in the SHRs compared to that of the WST rats (*p* < 0.01) and increased in response to the treatments (*p* < 0.05) (Fig. 3d).

Compromised global function in the SHRs is apparent from the delayed IVRT and increased Tei index. In the metoprolol- and famotidine-treated animals, the IVRT (*p* < 0.01) (Table 1) and Tei index (*p* < 0.01) (Fig. 3e) were lower than those of the SHRs. The magnitudes of the changes in the SHR-Fam and SHR-Met groups were comparable.

### Effect of famotidine and metoprolol on hypertrophy indicators

The serum and cardiac tissue lysate BNP levels were higher in the SHRs than in the WST rats (serum—*p* < 0.01 and cardiac tissue lysate—*p* < 0.01). The treatments significantly decreased the BNP levels (Fig. 4b).

The myocyte cross-sectional area was higher in the SHRs than in the WST rats (*p* < 0.01) and was reduced identically by the treatments (*p* < 0.01) (Fig. 4a, C).

The cardiac hypertrophy index, which was measured as the ratio of ventricular weight (mg) to body weight (g), was

higher in the SHRs than in the WST rats (*p* < 0.01) (Fig. 4d). The decreases in the hypertrophy index induced by famotidine (*p* < 0.01) and metoprolol were comparable.

### Effect of famotidine and metoprolol on cardiac fibrosis

Interstitial fibrosis was significantly higher in the SHRs than in the WST rats (*p* < 0.01) (Fig. 5a, b). A significant reduction in the stained area was found after famotidine treatment (*p* < 0.01) and was comparable to that of the metoprolol-treated group. Perivascular fibrosis, which was expressed as a function of the vessel lumen, was high in the SHRs compared to that in the WST rats (*p* < 0.01) (Fig. 5a, c). A decrease in perivascular fibrosis was observed in response to the treatments (*p* < 0.01).

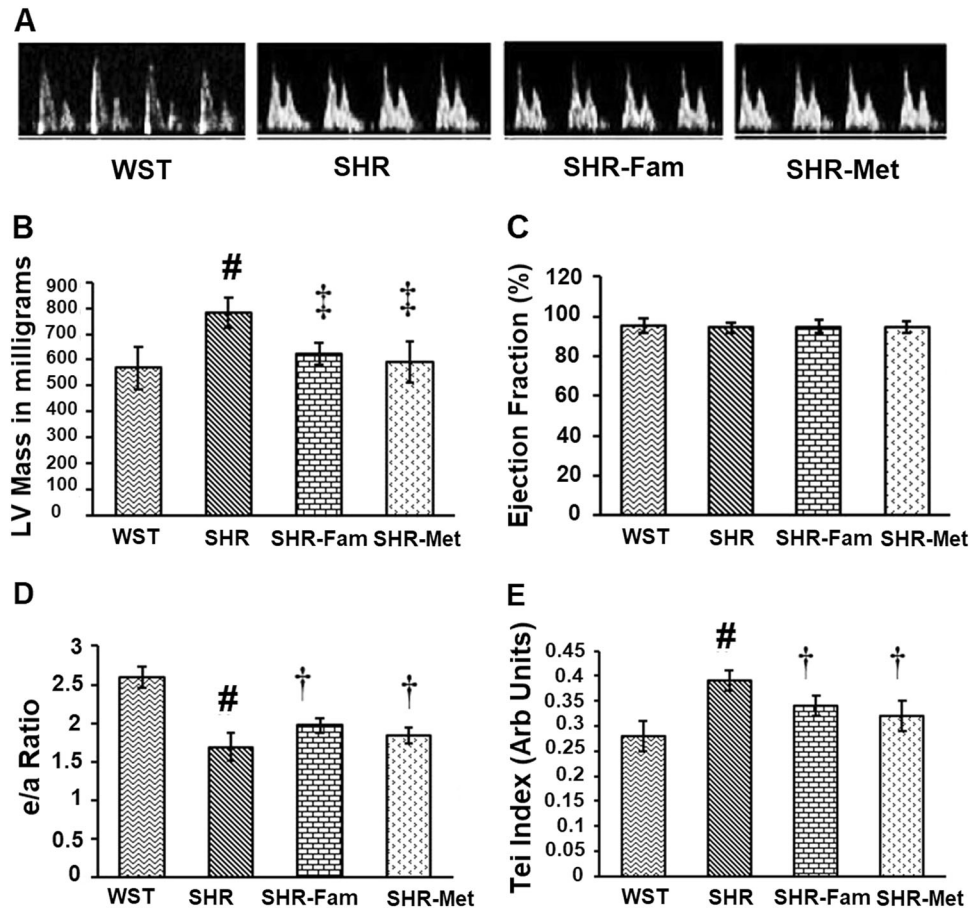
The hydroxyproline content was higher in the SHRs than in the WST rats (Fig. 5d). The famotidine and metoprolol interventions significantly reduced the hydroxyproline content (*p* < 0.05). The serum and cardiac tissue lysate PINP levels were higher in the SHRs than in the WST rats (serum—*p* < 0.05, cardiac tissue lysate—*p* < 0.01) (Fig. 5e). Famotidine treatment significantly reduced both the serum and cardiac tissue PINP levels (serum—*p* < 0.05, cardiac tissue lysate—*p* < 0.01) comparable to the metoprolol-treated group.

### Effects of famotidine and metoprolol on the histamine levels

The histamine levels were higher in the SHRs than in the WST rats (*p* < 0.01) (Fig. 6). Famotidine treatment

**Fig. 3** Cardiac performance in response to famotidine, with the metoprolol-treated group serving as the positive control.

**a** Representative picture of pulsed wave Doppler assessment of the mitral blood flow. **b** Graphical representation of the LV mass expressed in milligrams. **c** Graphical representation of the ejection fraction (EF) expressed as a percentage. **d** Graphical representation of the E/A ratio. **e** Graphical representation of the Tei index. The data are presented as the mean  $\pm$  SD. Variation was analyzed by one-way ANOVA followed by the Bonferroni post hoc test. \* $p < 0.05$  vs WST rats, # $p < 0.01$  vs WST rats, † $p < 0.05$  vs SHRs and ‡ $p < 0.01$  vs SHRs and ANOVA: Fig. 3b:  $p < 0.01$ , Fig. 3c:  $p = 0.89$ , Fig. 3d:  $p < 0.01$  and Fig. 3e:  $p < 0.05$  ( $n = 6$  per group)



significantly attenuated the histamine levels compared to those of the SHRs ( $p < 0.01$ ). The histamine levels were also reduced to a comparable extent in the metoprolol-treated group.

### Effects of famotidine and metoprolol on expression of proteins associated with maladaptive hypertrophy

The phosphorylated to total Akt ratio was higher in the SHRs than in the WST rats ( $p < 0.01$ ) (Fig. 7a). This ratio decreased after famotidine and metoprolol treatment ( $p < 0.01$ ). The Calcineurin-A levels were significantly higher in the SHRs than in the WST rats ( $p < 0.01$ ). Both famotidine and metoprolol treatment decreased the calcineurin-A levels ( $p < 0.05$ ), with no significant difference between treatments (Fig. 7b). The peroxiredoxin (PRX3) levels, which represent the mitochondrial antioxidant status, were lower in the SHRs than in the WST rats ( $p < 0.01$ ) (Fig. 7b). Famotidine and metoprolol enhanced the PRX3 levels compared to those of the untreated SHRs ( $p < 0.01$ ), and no significant difference was found between the treatments.

### Effect of histamine-2-receptor stimulation on cellular hypertrophy and delineation of the mechanism of action

Stimulation of H9c2 cells with histamine and the H2R agonist amthamine induced a significant dose-dependent increase in the expression and activity of the hypertrophic marker calcineurin. (Fig. 8a, d) The activity and expression of calcineurin after stimulation with the endogenous ligand histamine and the H2R agonist amthamine were comparable. Adenylate cyclase activity and the Akt and Erk phosphorylation statuses were also enhanced by both histamine and amthamine (Fig. 8b, c, e), indicating a role for adenylate cyclase-mediated Akt stimulation and Erk activation in mediating the hypertrophic response.

### Discussion

Left ventricular hypertrophy consequent to persistent hypertension is considered an independent risk factor for adverse cardiovascular events. Identification of novel mediators of hypertrophy can aid in the development of

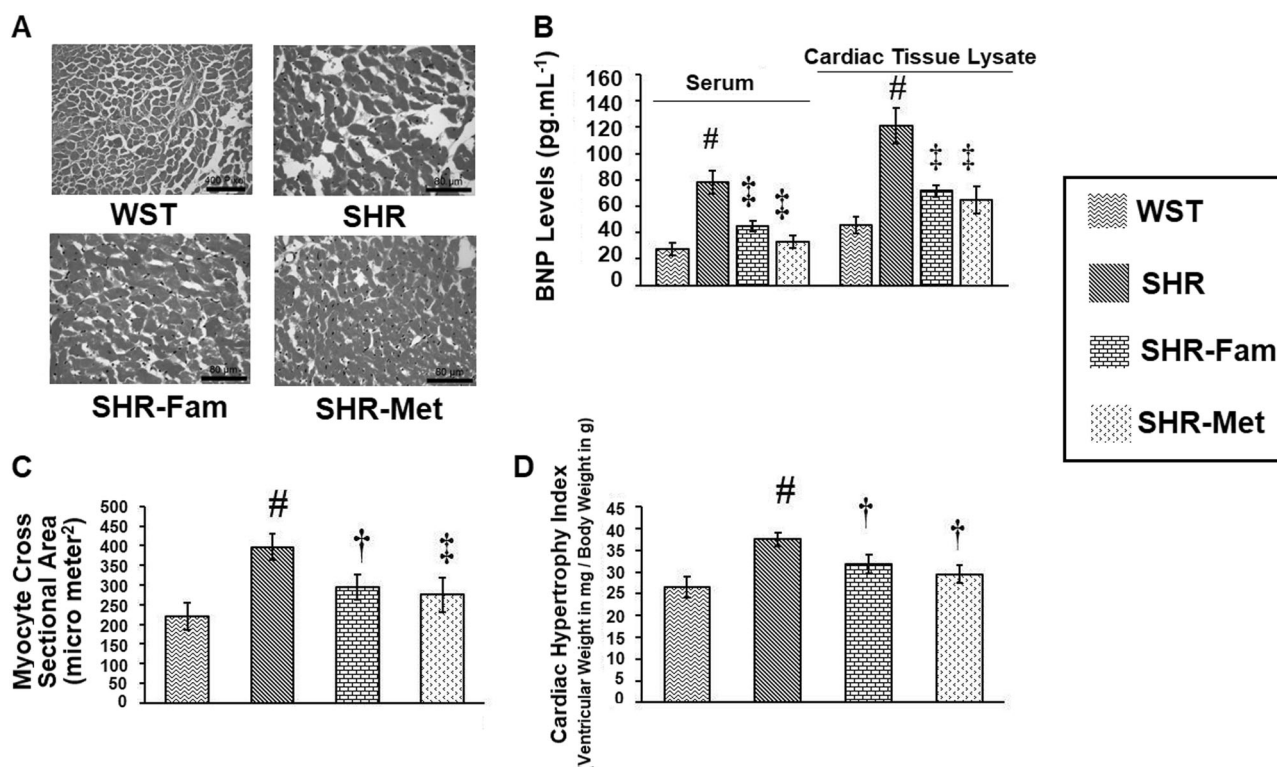


**Fig. 4** Effect of famotidine on the cardiac hypertrophy index, myocyte cross-sectional area and serum and myocardial BNP levels. The metoprolol-treated group served as the positive control. **a** Representative photomicrograph of histological sections of the myocardium stained with hematoxylin and eosin for calculation of the myocyte cross-sectional area. **b** Graphical representation of the serum and cardiac tissue lysate BNP levels expressed as pg/mL. **c** Graphical representation of the myocyte cross-sectional area expressed as  $\mu\text{M}^2$ .

**d** Graphical representation of the cardiac hypertrophy index (ventricular wt.mg/body wt.g). The data are presented as the mean  $\pm$  SD. Variation was analyzed by one-way ANOVA followed by the Bonferroni post hoc test. # $p < 0.01$  vs WSTs, ‡ $p < 0.01$  vs SHRs and † $p < 0.05$  vs SHRs. ANOVA: Fig. 4b: serum:  $p < 0.01$  and cardiac tissue lysate:  $p < 0.001$ , Fig. 4c:  $p < 0.05$  and Fig. 4d:  $p < 0.05$  ( $n = 6$  per group)

newer drugs to prevent progressive cardiac remodeling. The present study aimed to investigate the association of histamine and H2R with LVH progression and to prevent progressive cardiac remodeling by pharmacological inhibition of H2Rs in SHRs. The study highlights the association between histamine and LVH and the efficacy of H2R antagonism for modulation of cardiac structure and function.

Previous studies have reported the cardio-protective effects of H2R antagonists [4, 10], but an association of histamine and the H2R with hypertrophy has not been reported. This study showed that the myocardial histamine levels and degree of H2R expression increased with age in the SHRs but not in the normotensive Wistar rats (Fig. 1). The age-dependent increase in histamine and H2R expression supports the association of the variables with progressive cardiac remodeling. We observed a decrease in diastolic blood pressure in the SHRs treated with famotidine [9, 10]. No other reports have investigated the effect of H2R antagonists on blood pressure. In this study, we observed that the decrease in DBP induced by famotidine was not

significantly different than that of metoprolol; although, the decrease was not to the same extent as that induced by the  $\beta$ -blocker (Fig. 2). Administration of famotidine to the SHRs reduced myocardial fibrosis (Fig. 5) and improved diastolic function as assessed by pulsed wave Doppler (Table 1). Reductions in DBP are strongly influenced by ventricular diastole, and compliance can be the contributing factor in the regression of left ventricular hypertrophy, which makes these variables interdependent [23]. No significant change in SBP was seen with famotidine, whereas a decrease was observed with metoprolol. The regression of LVH by famotidine was comparable to that of metoprolol, as evident from the decrease in the LV mass and RWT (Fig. 3b and Table 1) and the hypertrophy index (Fig. 4d) and myocyte cross-sectional area (Fig. 4c). The increases in LVEDD and LVEDV correlated with the decrease in the LV mass (Table 1). The systolic function was comparable between the SHRs and WST rats and was unaffected by the treatments (Fig. 3c and Table 1).

Left ventricular diastolic function was assessed by echocardiography based on the early and late (E and A,



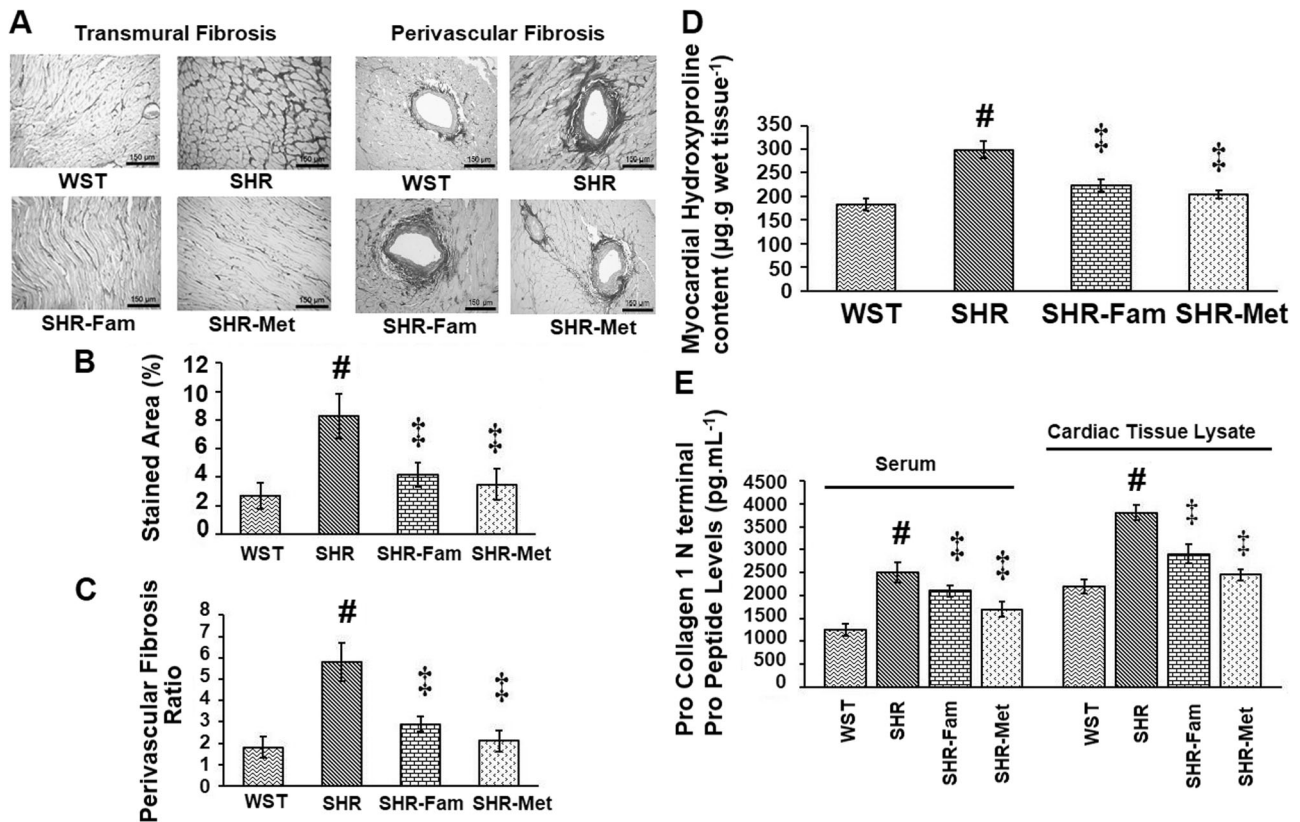


**Fig. 5** Effect of famotidine on cardiac fibrosis, with the metoprolol-treated group serving as the positive control. **a** Representative photograph of interstitial fibrosis and perivascular fibrosis. **b** Graphical representation of interstitial fibrosis. **c** Graphical representation of perivascular fibrosis expressed as a function of the vessel lumen. **d** Graphical representation of the hydroxyproline content. **e** Graphical

representation of the myocardial pro-collagen type 1 pro fiber levels. The data are presented as the mean ± SD. Variation was analyzed by one-way ANOVA followed by the Bonferroni post hoc test. <sup>#</sup>*p* < 0.01 vs WST rats and <sup>‡</sup>*p* < 0.01 vs SHRs. ANOVA: Fig. 5b: *p* < 0.01, Fig. 5c: *p* < 0.001, Fig. 5d: *p* < 0.01 and Fig. 5e: serum: *p* < 0.01 and cardiac tissue lysate: *p* < 0.001

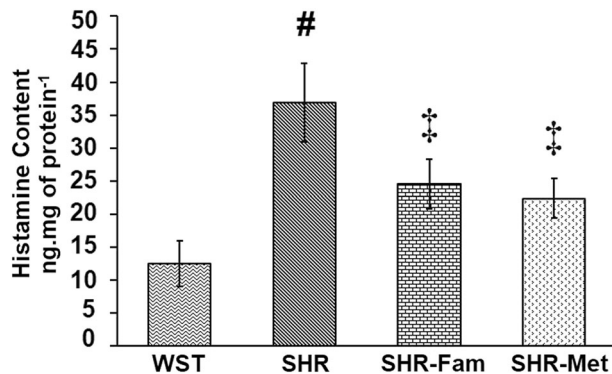


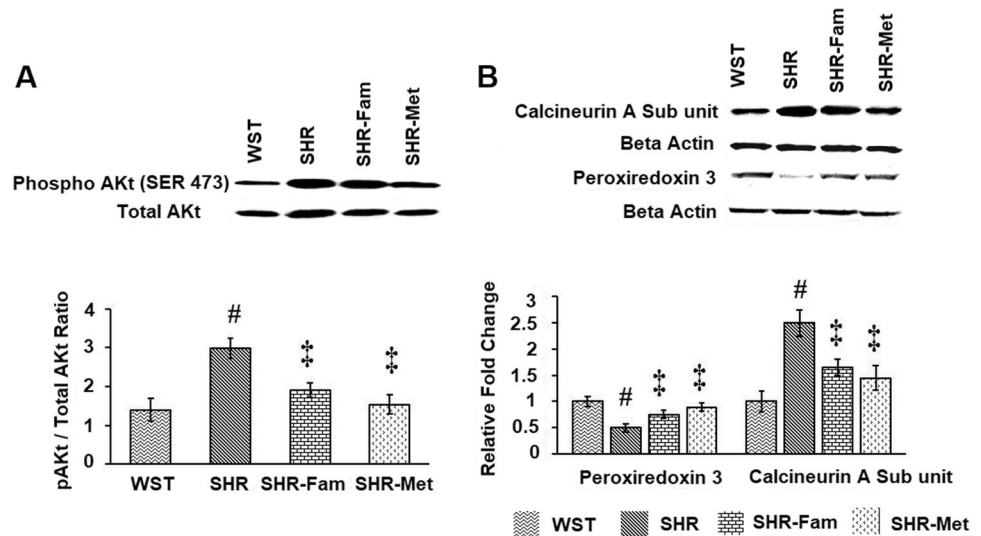
**Fig. 6** Effect of famotidine on the myocardial histamine levels (ng/mg protein), with the metoprolol-treated group serving as the positive control. The data are presented as the mean ± SD. Variation was analyzed by one-way ANOVA followed by the Bonferroni post hoc test. <sup>#</sup>*p* < 0.01 vs WST rats and <sup>‡</sup>*p* < 0.01 vs SHRs. ANOVA *p* < 0.01

the decrease in the A velocity and increase in the E/A ratio in response to metoprolol and famotidine indicate improvement of diastolic function, which is further supported by the normalized IVRT values (Table 1). The reduction in the Tei index in the treated animals suggest the possibility of reduced stiffness and improved relaxation and global myocardial performance (Fig. 3e).

Cardiac fibrosis is an integral feature of hypertrophy that is characterized by excessive deposition of collagen by fibroblasts (Fig. 5). The collagen content was assessed by measurement of the serum and myocardial hydroxyproline levels (Fig. 5d), the pro-collagen type 1 fiber levels (Fig. 5e), and histologically by picrosirius red staining (Fig. 5b, c). When compared to those of the WST rats, the markers of fibrosis in the SHRs were significantly higher, but attenuation of cardiac fibrosis was apparent in response to the treatments. Despite discrepant reports regarding the ability of metoprolol to reduce cardiac fibrosis, chronic metoprolol administration to the SHRs was associated with decreased cardiac fibrosis [16, 24]. The plasma and myocardial levels of natriuretic peptides are higher in concentric hypertrophy and correlate with its geometry and progression

respectively) mitral inflow velocities. Significant differences were observed in the E and A velocities and the E/A ratios in the SHR-C compared to those of the WST rats, suggesting the presence of diastolic dysfunction (Fig. 3d and Table 1). Although, the E velocity values were comparable,

**Fig. 7** Immunoblotting and densitometry analyses of molecular mediators of hypertrophy in the famotidine- and metoprolol-treated groups. **a** Densitometric analysis of the Akt phosphorylation levels with representative photographs of immunoblots. **b** Densitometric analysis of the calcineurin-A and PRX3 levels with representative photographs. The data are presented as the mean  $\pm$  SD. Variance was analyzed by one-way ANOVA followed by the Bonferroni post hoc test. # $p$  < 0.01 vs WST rats and † $p$  < 0.01 vs SHRs. ANOVA: Fig. 7A:  $p$  < 0.01 and Fig. 7B: PRX3— $p$  < 0.001, Calcineurin— $p$  < 0.05



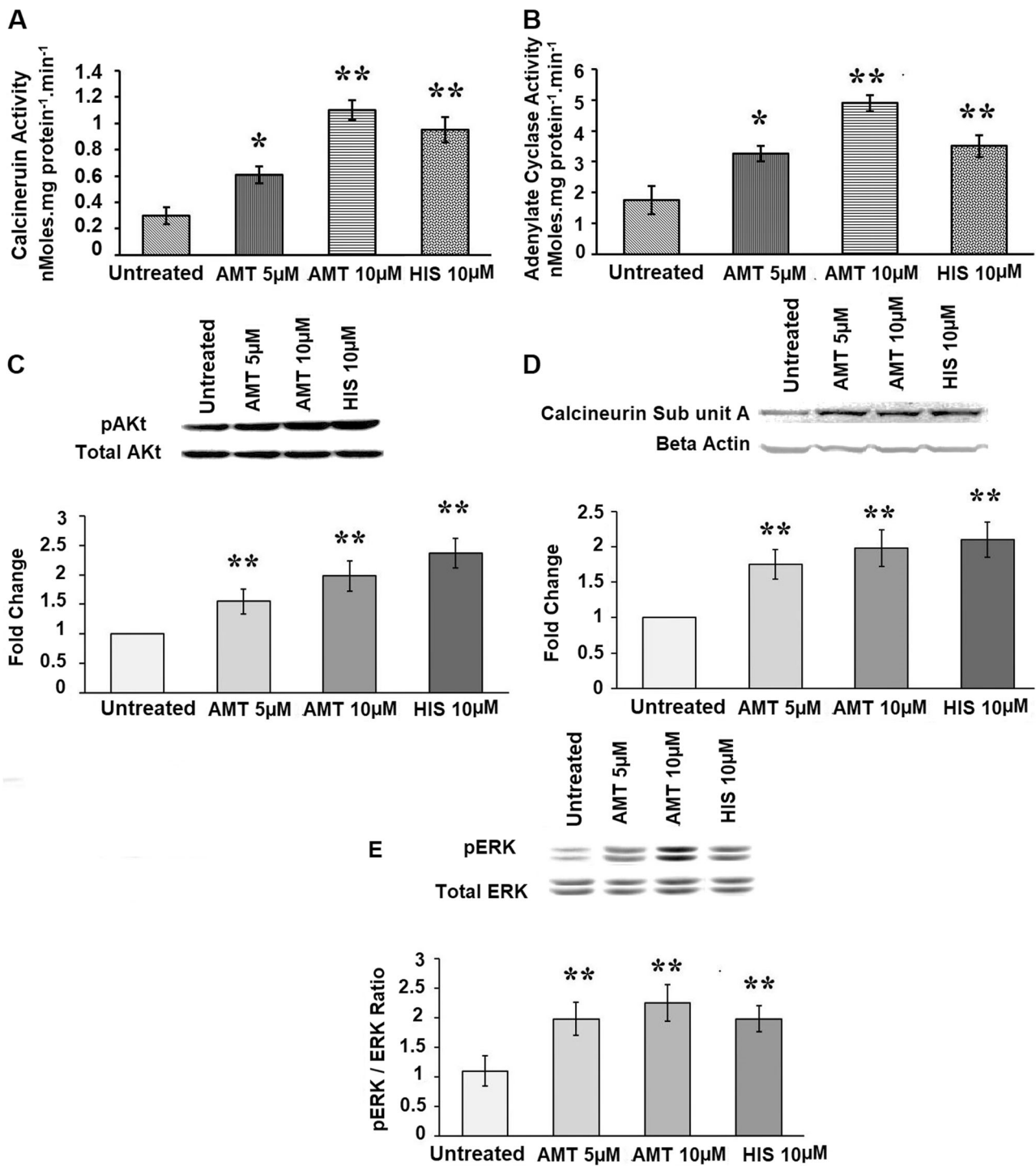
into failure [25]. The results from this study also indicate that the treatment induced a decrease in the morphological indices of LVH, including BNP activity (Fig. 4b). The magnitude of the reduction of these indices by famotidine was comparable with that of metoprolol.

Peroxiredoxin is a thioredoxin-based antioxidant protein that is abundant in the myocardium. PRX3 is mitochondria-specific, and studies with transgenic mice overexpressing peroxiredoxin3 have shown a lower risk of LV remodeling and progression into failure [26]. The PRX3 level in SHRs has been reported to be lower than that of Wistar rats and has been found to be involved in enhancing oxidative stress [27]. In accordance with this finding, we also found a significant reduction in the PRX3 level in the SHRs, which was restored upon treatment with metoprolol and famotidine (Fig. 7b). This positive cardiac response to both treatments is possibly the consequence of a reduction in oxidative stress in the hypertrophied myocardium and may be the key determinant for its pharmacological action.

The phosphatidylinositol 3-kinase (PI3K)/Akt (PKB) pathway is one prominent pathway by which hypertrophic mediators induce adverse cardiac remodeling. Upon activation, the phosphatidylinositol 3-kinase (PI3K)/Akt pathway leads to cardiac hypertrophy and increased collagen deposition [28]. Activation of the Akt signaling pathway imparts resistance against apoptosis and myocyte death. However, sustained activation of the Akt pathway leads to maladaptive hypertrophy and failure [28, 29]. Elevated Akt phosphorylation levels have been reported to be associated with adverse outcomes in several models of experimental and genetic hypertension [28]. Akt prevents the phosphorylation of glycogen synthase kinase-3 beta and attenuate its action [30, 31]. Reactivation of GSK-3 by various pharmacological compounds is known to prevent left ventricular remodeling [32]. In a hypertrophied heart, myocytes

experience beta adrenergic receptor-mediated activation of calcineurin, which is a key mediator of cardiac hypertrophy [33, 34]. This study showed elevated Akt phosphorylation and Calcineurin levels in the SHRs, as anticipated based on the pathological cardiac hypertrophy (Fig. 7a, b). The proportion of phosphorylated Akt and the calcineurin levels were significantly attenuated by metoprolol and famotidine, suggesting the possible involvement of the phosphatidylinositol 3-kinase (PI3K)/Akt and calcineurin-mediated pathways in the mediation of cardiac changes. In a mouse model of hypertrophy induced by transverse aortic constriction (TAC), studies inferred that myocardial H2R activation acted as an auxiliary regulator in the induction of calcineurin after TAC; a number of other stimuli, such as activation of the angiotensin and sympathetic systems, also contribute to the induction of calcineurin [9].

Targeting H2R and reducing histamine to prevent cardiac remodeling in chronic pressure overload are unexplored areas. Our earlier study suffered from the lacuna that the positive response to famotidine was not substantiated with the myocardial histamine levels and comparison with a known cardio-protective anti-hypertensive. This study showed that restoration of structural and functional efficiency by the H2R antagonist famotidine was comparable to that of the  $\beta$ -blocker metoprolol. A significant observation of the study is enhanced expression of the H2R and higher myocardial histamine levels in the SHRs than in the normotensive Wistar rats. The decrease in histamine in response to the treatments was associated with reverse remodeling, highlighting the role of histamine with chronic pressure overload hypertrophy. Beta-adrenergic receptors are expressed on mast cell membranes. Competition studies using [3 H]dihydroalprenolol ([3 H]DHA) revealed that ~84% of adrenergic receptors were the beta-2 subtype, whereas the remaining 16% were beta-1 adrenergic



receptors [35]. Although, the exact role of the beta-1 adrenergic receptor in modulating mast cell degranulation is not well understood, reports have suggested that stimulation of beta-2 adrenergic receptors cause mast cell stabilization and partially contribute to the anti-asthmatic effect of salbutamol and its analogues [36]. Hence, blocking the beta-1 adrenergic receptors can expose the remnant and abundant beta-2 adrenergic receptors to interact with elevated

catecholamines, resulting in mast cell stabilization. This effect may have contributed to the decrease in histamine levels by metoprolol treatment in the present study. Metoprolol is reported to have a minimal effect on mast cell degranulation when used in isolation compared to that of the ACE inhibitor combination [37].

After release from mast cells, histamine exerts auto-crine effects that regulate the mast cell degranulation

◀ **Fig. 8** Effect of histamine and histamine-2-receptor stimulation of H9c2 cardiomyoblasts on hypertrophic factors. **a** Calcineurin activity in H9c2 cardiomyoblasts upon exposure to Amthamine (AMT—5 and 10  $\mu$ M) and histamine (HIS —10  $\mu$ M) expressed as nMoles.mg-1.min-1. **b** Adenylate cyclase activity in H9c2 cardiomyoblasts upon exposure to AMT (5 and 10  $\mu$ M) and HIS (10  $\mu$ M) expressed as nMoles.mg-1.min-1. **c** Representative immunoblot showing the Akt phosphorylation rate in H9c2 cardiomyoblasts upon exposure to AMT (5 and 10  $\mu$ M) and HIS (10  $\mu$ M) and a graphical representation of the Akt phosphorylation rate in H9c2 cardiomyoblasts upon exposure to AMT (5 and 10  $\mu$ M) and HIS (10  $\mu$ M). **d** Representative immunoblot showing Calcineurin-A expression in H9c2 cardiomyoblasts upon exposure to AMT (5 and 10  $\mu$ M) and HIS (10  $\mu$ M) and a graphical representation of Calcineurin-A expression in H9c2 cardiomyoblasts upon exposure to AMT (5 and 10  $\mu$ M) and HIS (10  $\mu$ M). **e** Representative immunoblot showing the ERK phosphorylation rate in H9c2 cardiomyoblasts upon exposure to AMT (5 and 10  $\mu$ M) and HIS (10  $\mu$ M) and a graphical representation of the ERK phosphorylation rate in H9c2 cardiomyoblasts upon exposure to AMT (5 and 10  $\mu$ M) and HIS (10  $\mu$ M). All of the experiments were conducted in triplicate ( $n = 3$ ). The data are represented as the mean  $\pm$  SD. Variance was analyzed by one-way ANOVA followed by the Bonferroni post hoc test. \* $p < 0.05$  vs untreated cells and \*\* $p < 0.01$  vs untreated cells. ANOVA: Fig. 8A:  $p < 0.05$ , Fig. 8B:  $p < 0.01$ , Fig. 8C:  $p < 0.01$ , Fig. 8D:  $p < 0.05$  and Fig. 8E:  $p < 0.001$

mediated by the H2 receptor [38]. Histamine is also known to increase the chemotaxis of mast cells, thereby promoting their tissue density [39]. This proposition is supported by studies using roxatidine in the human mast cell line-1 (HMC-1) activated by compound 48/80 to induce degranulation. H2 blockers inhibit the NF $\kappa$ B and P38 MAPK pathways, thereby preventing degranulation [40]. In light of these findings, famotidine may block the autocrine effects of histamine on mast cells, thereby preventing their degranulation.

Additionally, when cultured H9c2 cardiac cells were used to examine the role of histamine in mediating the hypertrophic response, we observed that supplementation with histamine and stimulation of H2Rs with their specific agonist amthamine induced dose-dependent activation of various mediators of cardiac hypertrophy, such as calcineurin-A, pAkt, and pERK (Fig. 8). These findings further support the contention that histamine can induce H2R-mediated cardiac remodeling. In conclusion, the study provides impetus for a novel approach in the management of cardiac hypertrophy and associated cardiovascular ailments.

**Acknowledgements** The authors gratefully acknowledge the Indian Council for Medical Research for financial support for the study and the Research Fellowship to Ajay Godwin Potnuri.

### Compliance with ethical standards

**Conflict of interest** The authors declare that they have no conflict of interest.

## References

- Katholi RE, Couri DM. Left ventricular hypertrophy: major risk factor in patients with hypertension: update and practical clinical applications. *Int J Hypertens* 2011; 2011. <https://doi.org/10.4061/2011/495349>
- Tin LL, Beevers DG, Lip GYH. Hypertension, left ventricular hypertrophy, and sudden death. *Curr Cardiol Rep*. 2002;4:449–57.
- Gradman AH, Alfayoumi F. From left ventricular hypertrophy to congestive heart failure: management of hypertensive heart disease. *Prog Cardiovasc Dis*. 2006;48:326–41.
- Leary PJ, Barr RG, Bluemke DA, Bristow MR, Kronmal RA, Lima JA, et al. H2 receptor antagonists and right ventricular morphology: the MESA right ventricle study. *Ann Am Thorac Soc*. 2014;11:1379–86.
- Levick SP, McLarty JL, Murray DB, Freeman RM, Carver WE, Brower GL. Cardiac mast cells mediate left ventricular fibrosis in the hypertensive rat heart. *Hypertension*. 2009;53:1041–7.
- Laine P, Kaartinen M, Penttilä A, Panula P, Paavonen T, Kovanen PT. Association between myocardial infarction and the mast cells in the adventitia of the infarct-related coronary artery. *Circulation*. 1999;99:361–9.
- Zdravkovic V, Pantovic S, Rosic G, Tomic-Lucic A, Zdravkovic N, Colic M, et al. Histamine blood concentration in ischemic heart disease patients. *Biomed Res Int*. 2011;2011:e315709.
- Del Valle J, Gantz I. Novel insights into histamine H2 receptor biology. *Am J Physiol*. 1997;273:G987–996.
- Zeng Z, Shen L, Li X, Luo T, Wei X, Zhang J, et al. Disruption of histamine H2 receptor slows heart failure progression through reducing myocardial apoptosis and fibrosis. *Clin Sci*. 2014;127:435–48.
- Potnuri AG, Allakonda L, Appavoo A, Saheera S, Nair RR. Targeting histamine-2 receptor for prevention of cardiac remodeling in chronic pressure overload. *Int J Cardiol*. 2016;202:831–3.
- George T, Ajit MS, Abraham G. Beta blockers & left ventricular hypertrophy regression. *Indian Heart J*. 2010;62:139–42.
- Berry JM, Naseem RH, Rothermel BA, Hill JA. Models of cardiac hypertrophy and transition to heart failure. *Drug Discov Today Dis Models*. 2007;4:197–206.
- Purushothaman S, Nair RR, Harikrishnan VS, Fernandez AC. Temporal relation of cardiac hypertrophy, oxidative stress, and fatty acid metabolism in spontaneously hypertensive rat. *Mol Cell Biochem*. 2011;351:59–64.
- Pradeepkumar Singh L, Kundu P, Ganguly K, Mishra A, Swarnakar S. Novel role of famotidine in downregulation of matrix metalloproteinase-9 during protection of ethanol-induced acute gastric ulcer. *Free Radic Biol Med*. 2007;43:289–99.
- Ahmadi A, Ebrahimzadeh MA, Ahmad-Ashrafi S, Karami M, Mahdavi MR, Saravi SSS. Hepatoprotective, antinociceptive and antioxidant activities of cimetidine, ranitidine and famotidine as histamine H2 receptor antagonists. *Fundam Clin Pharmacol*. 2011;25:72–79.
- Chan V, Fenning A, Hoey A, Brown L. Chronic  $\beta$ -adrenoceptor antagonist treatment controls cardiovascular remodeling in heart failure in the aging spontaneously hypertensive rat. *J Cardiovasc Pharmacol*. 2011;58:424–31.
- Annapurna A, Challa SR, Prakash GJ, Viswanath RK. Therapeutic potential of sulindac against ischemia-reperfusion-induced myocardial infarction in diabetic and nondiabetic rats. *Exp Clin Cardiol*. 2008;13:66–70.

18. Potnuri AG, Kondru SK, Samudrala PK, Allakonda L. Prevention of adriamycin induced cardiotoxicity in rats — A comparative study with subacute angiotensin-converting enzyme inhibitor and nonselective beta blocker therapy. *IJC Metab Endocr.* 2017;14:59–64.
19. Escudero EM, Hurtado MCC, de, Pérez NG, Tufare AL. Echocardiographic assessment of left ventricular midwall mechanics in spontaneously hypertensive rats. *Eur Heart J - Cardiovasc Imaging.* 2004;5:169–75.
20. Tiligada E, Aslanis D, Delitheos A, Varonos D. Changes in histamine content following pharmacologically-induced mast cell degranulation in the rat conjunctiva. *Pharmacol Res.* 2000;41:667–70.
21. Reddy GK, Enwemeka CS. A simplified method for the analysis of hydroxyproline in biological tissues. *Clin Biochem.* 1996;29:225–9.
22. Rius RA, Mollner S, Pfeuffer T, Peng Loh Y. Developmental changes in Gs and Golf proteins and adenylyl cyclases in mouse brain membranes. *Brain Res.* 1994;643:50–8.
23. Zhang K, Chen J, Liu Y, Wang T, Wang L, Wang J, et al. Diastolic blood pressure reduction contributes more to the regression of left ventricular hypertrophy: a meta-analysis of randomized controlled trials. *J Hum Hypertens.* 2013;27:698–706.
24. Sun T, Shen L-H, Chen H, Li H-W, Guo C-Y, Li Z-Z, et al. Effects of carvedilol and metoprolol on cardiac fibrosis in rats with experimental myocardial infarction. *Zhonghua Xin Xue Guan Bing Za Zhi.* 2008;36:68–71.
25. Kohno M, Horio T, Yokokawa K, Yasunari K, Ikeda M, Minami M, et al. Brain natriuretic peptide as a marker for hypertensive left ventricular hypertrophy: changes during 1-year antihypertensive therapy with angiotensin-converting enzyme inhibitor. *Am J Med.* 1995;98:257–65.
26. Matsushima S, Ide T, Yamato M, Matsusaka H, Hattori F, Ikeuchi M, et al. Overexpression of mitochondrial peroxiredoxin-3 prevents left ventricular remodeling and failure after myocardial infarction in mice. *Circulation.* 2006;113:1779–86.
27. Tanito M, Nakamura H, Kwon Y-W, Teratani A, Masutani H, Shioji K, et al. Enhanced oxidative stress and impaired thioredoxin expression in spontaneously hypertensive rats. *Antioxid Redox Signal.* 2004;6:89–97.
28. Taniyama Y, Ito M, Sato K, Kuester C, Veit K, Tremp G, et al. Akt3 overexpression in the heart results in progression from adaptive to maladaptive hypertrophy. *J Mol Cell Cardiol.* 2005;38:375–85.
29. Fujio Y, Nguyen T, Wencker D, Kitsis RN, Walsh K. Akt promotes survival of cardiomyocytes in vitro and protects against ischemia-reperfusion injury in mouse heart. *Circulation.* 2000;101:660–7.
30. De Sarno P, Li X, Jope RS. Regulation of Akt and glycogen synthase kinase-3 beta phosphorylation by sodium valproate and lithium. *Neuropharmacology.* 2002;43:1158–64.
31. Atkins RJ, Dimou J, Paradiso L, Morokoff AP, Kaye AH, Drummond KJ, et al. Regulation of glycogen synthase kinase-3 beta (GSK-3 $\beta$ ) by the Akt pathway in gliomas. *J Clin Neurosci J Neurosurg Soc Australas.* 2012;19:1558–63.
32. Fujita A, Takahashi-Yanaga F, Morimoto S, Yoshihara T, Arioka M, Igawa K, et al. 2,5-Dimethylcelecoxib prevents pressure-induced left ventricular remodeling through GSK-3 activation. *Hypertens Res.* 2017;40:130–9.
33. Soesanto W, Lin H-Y, Hu E, Lefler S, Litwin SE, Sena S, et al. Mammalian target of rapamycin is a critical regulator of cardiac hypertrophy in spontaneously hypertensive rats. *Hypertension.* 2009;54:1321–7.
34. Lunde IG, Kvaløy H, Austbø B, Christensen G, Carlson CR. Angiotensin II and norepinephrine activate specific calcineurin-dependent NFAT transcription factor isoforms in cardiomyocytes. *J Appl Physiol.* 2011;111:1278–89.
35. Marquardt DL, Wasserman SI. Characterization of the rat mast cell beta-adrenergic receptor in resting and stimulated cells by radioligand binding. *J Immunol.* 1982;129:2122–7.
36. Peachell P. Regulation of mast cells by beta-agonists. *Clin Rev Allergy Immunol.* 2006;31:131–42.
37. Nassiri M, Babina M, Dölle S, Edenharter G, Ruëff F, Worm M. Ramipril and metoprolol intake aggravate human and murine anaphylaxis: evidence for direct mast cell priming. *J Allergy Clin Immunol.* 2015;135:491–9.
38. Carlos D, Sá-Nunes A, de Paula L, Matias-Peres C, Jamur MC, Oliver C, et al. Histamine modulates mast cell degranulation through an indirect mechanism in a model IgE-mediated reaction. *Eur J Immunol.* 2006;36:1494–503.
39. Keles N, Yavuz Arican R, Coskun M, Elpek GO. Histamine induces the neuronal hypertrophy and increases the mast cell density in gastrointestinal tract. *Exp Toxicol Pathol J Ges Toxikol Pathol.* 2012;64:713–6.
40. Lee M, Lee NY, Chung K-S, Cheon S-Y, Lee K-T, An H-J. Roxatidine attenuates mast cell-mediated allergic inflammation via inhibition of NF- $\kappa$ B and p38 MAPK activation. *Sci Rep.* 2017;7:41721.